Renewable Energy 225 (2024) 120317

Contents lists available at ScienceDirect

Renewable Energy

journal homepage: www.elsevier.com/locate/renene

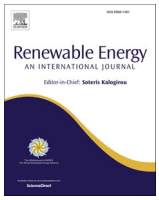

Quantifying the impact of inverter clipping on photovoltaic performance and soiling losses

Leonardo Micheli [a,*], Matthew Muller [b], Marios Theristis [c], Greg P. Smestad [d], Florencia Almonacid [e], Eduardo F. Fernández [e]

[a] Department of Astronautic, Electric and Energy Engineering (DIAEE), Sapienza University of Rome, Rome, 00184, Italy
[b] National Renewable Energy Laboratory (NREL), Golden, 80401, CO, USA
[c] Sandia National Laboratories, Albuquerque, 87185, NM, USA
[d] Sol Ideas Technology Development, San José, 95150, CA, USA
[e] Advances in Photovoltaic Technology (AdPVTech), CEACTEMA, University of Jaén (UJA), Jaén, 23071, Spain

ARTICLE INFO

Keywords:
Photovoltaics
Inverter clipping
Inverter loading ratio
Soiling
Operation and maintenance

ABSTRACT

It is commonly assumed that cleaning photovoltaic (PV) modules is unnecessary when the inverter is undersized because clipping will sufficiently mask the soiling losses. Clipping occurs when the inverter's AC size is smaller than the overall modules' DC capacity and leads to the conversion of only part of the PV-generated DC energy into AC. This study evaluates the validity of this assumption, theoretically investigating the current magnitude of clipping and its effect on soiling over the contiguous United States. This is done by modelling energy yield, clipping and soiling across a grid of locations. The results show that in reality, under the current deployment trends, inverter undersizing minimally affects soiling, as it reduces these losses by no more than 1%$_{absolute}$. Indeed, clipping masks soiling in areas where losses are already low, whereas it has a negligible effect where soiling is most significant. However, the mitigation effects might increase under conditions of lower performance losses or more pronounced inverter undersizing. In any case, one should take into account that degradation makes clipping less frequent as systems age, also decreasing its masking effect on soiling. Therefore, even if soiling was initially mitigated by the inverter undersizing, its effect would become more visible with time.

1. Introduction

Soiling consists of the accumulation of dust, dirt, and particles on the surface of photovoltaic (PV) modules. It reduces the intensity of the irradiance reaching the photovoltaic material and, therefore, converted into electricity. Soiling affects, with variable severity, PV systems worldwide, and can result in significant economic losses [1]. Being a reversible loss mechanism, soiling can be mitigated either by prevention or removal through a number of strategies [2–4]. These have costs that can affect the capital and/or operating expenditure of a PV system. Therefore, any soiling mitigation solution has to be planned to maximize the difference between revenues from the recovered energy and their costs. For example, cleanings, the most common soiling mitigation strategy nowadays, should not be performed in proximity of rain events. Rainfalls, indeed, can wash off soiling from the PV modules at no cost, reducing the amount of recoverable energy from artificial cleanings and, therefore, their profitability [5].

In order to facilitate the cleaning optimization of field PV systems, several cleaning optimization algorithms have been proposed in literature. Cristaldi et al. [6] recommended cleaning the PV modules as soon as the losses are higher than the cleaning costs. Jones et al. [7] calculated the optimal cleaning interval for a PV system in Saudi Arabia by minimizing the sum of cleaning costs and revenue losses. Besson et al. [8] proposed a method based on the difference between revenues and costs, which was also applied to bifacial modules by Luque et al. [9]. You et al. [10] identified the optimal cleaning frequency for different PV sites by maximizing the net present value, a metric that evaluates the profitability of an investment.

The aforementioned methods take into account various factors that can influence the operation and maintenance (O&M) and cleaning decisions, such as the weather and precipitation pattern, the soiling accumulation rate, the price of electricity, the cleaning cost, and the energy loss. However, a well-known factor has so far been overlooked in cleaning optimization studies. This is the undersizing of the inverter,

* Corresponding author.
E-mail address: leonardo.micheli@uniroma1.it (L. Micheli).

https://doi.org/10.1016/j.renene.2024.120317
Received 22 September 2023; Received in revised form 7 March 2024; Accepted 11 March 2024
Available online 12 March 2024

which is often intentionally designed to have lower capacity compared to the nominal DC capacity of the PV modules. This practice allows minimizing life-cycle costs and is occasionally required by regulators to smooth grid integration [11]. A report published by Bolinger et al. [12] showed that, in the U.S., the inverter undersizing has substantially increased over the last decade. Indeed, they found that the median inverter size decreased from being 20% lower than the DC capacity of the PV plants in 2010 to 34% in 2020.

When the DC energy is larger than the inverter size, a phenomenon known as "clipping" occurs [13]. The inverter saturates and, therefore, the excess DC energy is masked and not converted into AC. Because of this masking effect, inverter undersizing has been often suggested as practical soiling mitigation strategy [14]. Indeed, the soiling losses are not visible from the AC side during clipping if they are not bigger than the difference between the energy rating of the modules and the capacity of the inverter [11]. However, no study has yet quantified the magnitude of soiling mitigation achievable through inverter clipping.

In light of these considerations, this work aims to provide an analytical answer to whether the current inverter undersizing level is masking losses enough to make additional soiling mitigation activities no longer needed. This is done by investigating the impact of inverter clipping on PV performance, with a particular focus on soiling losses, across the contiguous U.S. The analysis is conducted by modelling the PV performance and the soiling distribution using gridded weather data, referenced models and actual information on the typical PV installations. The results of this work make it possible to evaluate weather and irradiance conditions that either favour or hinder clippings, and to quantify the masking effect of clipping on soiling in regions experiencing different levels of soiling loss. Ultimately, this research aims to address the question of whether clipping alone is always a viable solution that renders other soiling mitigation actions, such as cleaning, unnecessary.

2. Methodology

The analysis presented in this work followed the process depicted in Fig. 1, implemented in Python 3.7. The main steps of the methodology included the modelling of the PV performance (described in Section 2.1), the quantification of clipping (2.2) and the estimation of soiling (2.3).

The analysis considered a grid of locations across the contiguous U.S. spanning between latitudes from 25.5° to 49.0° and longitudes from −124.375° to −67.5°. Only inland locations were considered, excluding sea/ocean locations. For each site, the time series of DC and AC power output and soiling losses were estimated using.

- irradiance and weather data from NSRDB [15].
- daily precipitation data from PRISM [16].
- daily mean particulate matter (PM_{10} and $PM_{2.5}$) time series generated from MERRA-2 data [17,18].

The maps were generated using the Cartopy package [19]. Linear interpolation was employed to produce the surface maps from the abovementioned grid. The climate of each location was identified according to the Köppen-Geiger classification [20–22] using the kgcPy library [23].

2.1. PV performance model

Power outputs were calculated for a 0.5° × 0.65° grid of points over the contiguous U.S. using the PVWatts DC power model [24] from pvlib-python [25]. Irradiance and weather data were downloaded at a 5-min interval from NSRDB [15] for the period between 2018 and 2020. The models presented by Refs. [26,27] were used to calculate the ground diffuse and sky diffuse components of irradiance, with the albedo set to the pvlib python default value of 0.25 [25]. The Sandia temperature model was employed to calculate the temperature of the photovoltaic cell, assuming open-rack glass/polymer modules [28]. The analysis was conducted considering monofacial silicon modules. The power temperature coefficient was set to −0.34%/°C [29]. The angle of incidence losses were modelled using the procedure in Ref. [30], and 10% losses were applied to convert DC power into an AC output, in addition to a 95% inverter efficiency (i.e. 5% inverter loss).

In 2021, approximately 75% of the utility-scale PV capacity was comprised of tracked systems, with the majority of these employing horizontal single-axis tracking (HSAT) mechanisms [12]. Therefore, modules were modelled as mounted on a horizontal axis aligned along the north-south direction, moving east to west. The maximum rotation angle was set to 60°. Backtracking capabilities were simulated, assuming a ground coverage ratio of 0.286. This is the default value in pvlib-python [25], and corresponds to a tracked system made of 2 m wide modules mounted in rows spaced at 7 m. The HSAT movement was modelled using the methodology proposed in Ref. [31]. In addition, a fixed tilt configuration was also considered, assuming latitude tilt and southward orientation.

The DC energy output of a PV system at a given location at time t was calculated as:

$$E_{DC}(t) = E(t) \bullet r_s(t) \bullet (1 - PV_{loss}) \bullet (1 + r_d)^n \quad (1)$$

where E(t) is the lossless DC energy yield calculated using the aforementioned PVWatts DC power model [24], r_s is the soiling ratio, equal to 1 – soiling loss, PV_{loss} is the system loss, considered in the reference scenario fixed at 10% [32], r_d is the system performance loss rate (expressed as a negative value) and the n is number of years since installation.

As shown in equation (1), the effect of long-term irreversible performance loss on clipping frequency is also taken into account. Indeed, one can expect clipping to become less frequent as performance losses worsen while the system components age. In this work, a linear −0.75 %/year performance loss rate (r_d) was assumed based on the latest results from the PV Fleet Performance Data Initiative [33].

2.2. Clipping model

The inverter's undersizing is typically quantified using the DC-to-AC ratio, or inverter-loading ratio (ILR). This expresses the ratio between the DC capacity and the inverter's AC power rating. So, the inverter is undersized if ILR >1. According to Bolinger et al. [12], in 2020, the median ILR for PV systems installed in the U.S. reached 1.34, for both tracked and fixed configurations, with 20th and 80th percentiles of 1.26 and 1.45.

Inverter clipping occurs when the DC power is greater than the AC

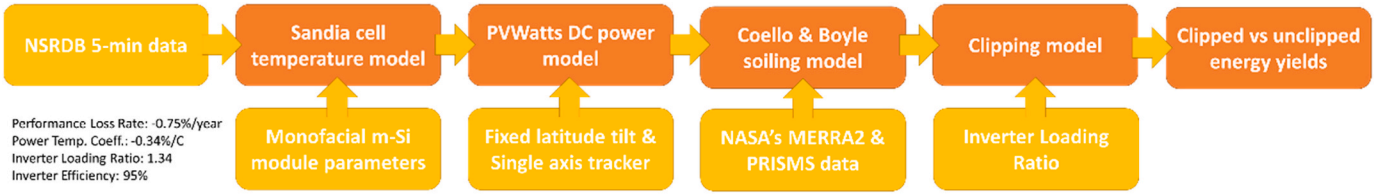

Fig. 1. Workflow describing the employed methodology and the data sources.

inverter's production capacity. When clipping, the PV power time series flattens at or near the inverter's capacity [34]. This is reproduced in this work using the model shown in the left plot of Fig. 2, which can be expressed as:

$$E_{AC}(t) = \min\left(E_{DC}(t) \bullet \eta_{inv}, E_{DCstd} \bullet ILR^{-1}\right) \quad (2)$$

Where E_{DCstd} is the nominal DC energy output produced by the system under standard test conditions, E_{AC} is the AC energy output and η_{inv} is the inverter's efficiency, fixed to 95% in this case. In the example of the left plot of Fig. 2, a 5% soiling on the DC side causes a loss of only 2.3% on the AC power output, because of the 1.34 DC to AC ratio. This way, the soiling losses are visible during the first and the last hours of the day only and have no effects on the peak production period.

The clipping model presented here was validated using data from two of the sites available in Ref. [34]. These systems are mounted in a fixed configuration, facing southward. One site is located in the north-east of the U.S. (Massachusetts), and one in the southwest (California). Clipping occurs for at least 1 h in between 12% and 30% of the days, with the highest percentages in California. When the modelled data are compared to the actual data, an average mean absolute error of 7.9% is found (irradiance <100 W/m^2 and DC power <50 W filtered out as in Ref. [35]). This value is in line with the overall uncertainty range reported by the IEA PVPS Task 13 experts [36] and is slightly above the median error found in a recent PV modelling round robin [35]. Differently from the latter, however, which employed irradiance measured by laboratory-standard sensors, this work made use of satellite-derived irradiance data. These are indeed essential for a systematic large-scale analysis and for the generation of maps, but are exposed to higher uncertainties compared to well-maintained ground sensors. The 5-min NSRDB data, in particular, have returned root-mean-square-error of 14–30% when compared with the ground-measurements of six Surface Radiation Budget Network stations [37]. In light of this additional uncertainty, the error found for the present method can be considered reasonable and in line with the existing literature.

The actual and modelled clipping data for two representative days at these sites are shown in the right side plots of Fig. 2. As it can be seen, the actual AC performance flattens in the central hours of the day (red line with cross markers). The model is able to reproduce that profile (bold black line with round markers) and to also simulate the performance for conditions of no clipping (grey dotted line). The energy masked by clipping (E_{clip}) can be therefore calculated as:

$$E_{clip}(t) = E_{DC}(t) \bullet \eta_{inv} - E_{AC}(t) \quad (3)$$

As mentioned, the full-scale analysis was based on 5-min energy yield data. Data frequency is indeed known to be key for inverter clipping studies. The use of larger time intervals has been found to cause underestimation of the clipped energy. A work conducted on a potential solar site in Oak Ridge (Tennessee, U.S.) found that using hourly data in place of 1-min data led to underestimation of clipping of 1.5% and 2.4% for ILR of 1.25 and 1.50, respectively [38]. A 2.3% error was found when estimating the 2019 annual energy yield of a 1.3 ILR-system in Northbridge (Massachusetts, U.S.) using hourly instead of sub-hourly data [39]. Researchers from NREL mapped the clipping modelling error when 30-min data are shown in place of 1-min data, showing errors ranging from −0.6 to 1.6% [40]. The 5-min interval is still expected to cause some underestimation in the quantification of clipping [39]. However, it was selected because it represents the smallest time interval available on NSRDB [15].

2.3. Soiling model

Various models have been presented in the literature to simulate the daily soiling loss profile of a PV system. For the present work, the model proposed by Coello and Boyle [41] was considered. This model was selected because it was originally developed specifically for the U.S.

In this work, the Coello and Boyle model was run with hourly data from NASA's MERRA-2 [17,18], at 0.5° × 0.65° resolution, estimating the accumulated soiling mass by assuming a constant settling velocity. The PM_{10} and $PM_{2.5}$ concentrations were calculated using the procedure recommended by the MERRA-2 guidelines [42,43]. The accumulated soiling mass was calculated at a daily interval and, as in the original model, reset each time the daily rainfall was greater than 1 mm/day. The rainfall data were downloaded at a daily interval from the PRISM database [16] (same resolution as MERRA-2). Lastly, the soiling time series was converted into the same 5-min interval as the energy yield by assuming it linearly builds up during the day. Therefore, the solar angle

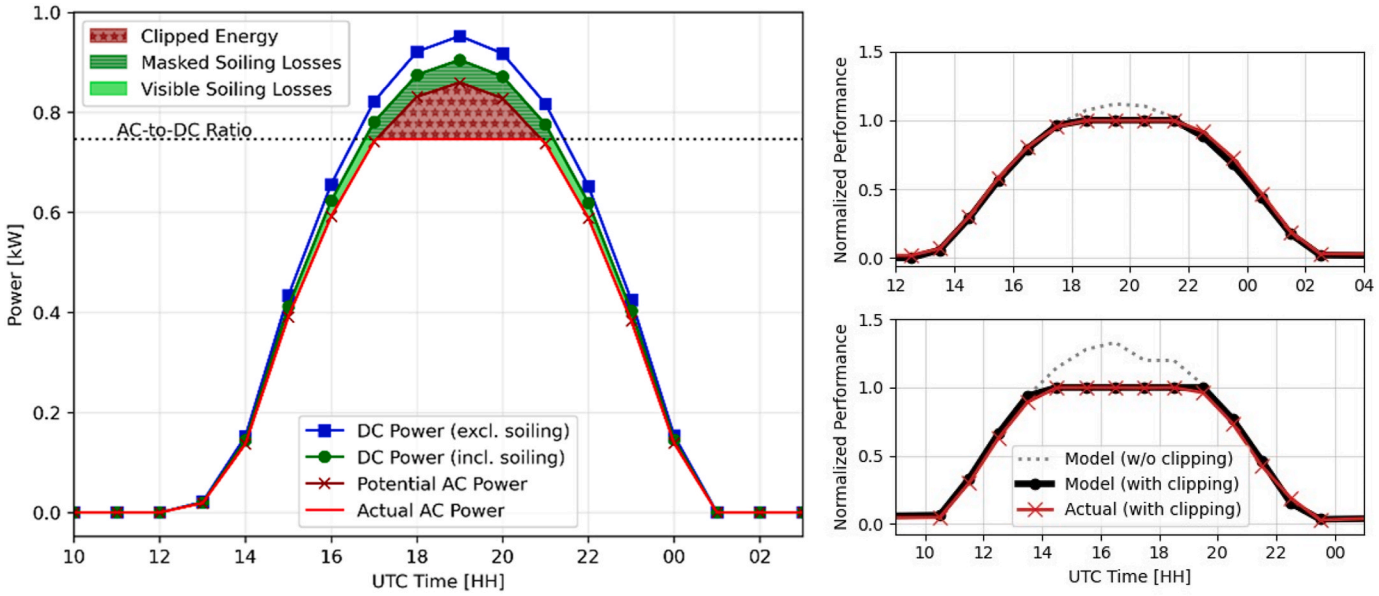

Fig. 2. Left: Simulation of inverter clipping on 1kW$_{DC}$ fixed-tilt system in Broomfield, Colorado, on March 20, 2015. The following losses were considered: 10% DC losses (excluding soiling), 5% soiling losses, 5% inverter losses. The DC to AC ratio was set to 1.34. After clipping, soiling losses reduce the actual AC power by 2.3%. Total clipped DC energy: 6.9%. Right: modelled and actual clipping occurring over a day at the two PV sites in the U.S. For better clarity, markers are shown at an hourly interval.

of incidence effect on soiling was not considered [44]. The same soiling loss profile, calculated assuming a latitude tilt, was applied to both fixed and tracked PV module configurations.

The Coello and Boyle model was tested against a new set of soiling data measured at Sandia National Laboratories in between the second half of 2015 and the end of 2019. In this case, a split-cell reference cell was mounted at 30°. One of the half-cells was cleaned twice per week, whereas the other half-cell was left to soil naturally. Soiling was expressed through the soiling ratio, which quantifies the fraction of energy left after the soiling loss. It was calculated as the ratio between the short-circuit currents of the two half-cells, under the assumption that the fill factor and open circuit voltage do not change significantly with a reduction in irradiance caused by soiling. A plot of the validation results is shown in Fig. 3. As can be seen, using the original settling deposition velocities would lead to an underestimation of the losses (i.e., overestimation of the soiling ratio). This is particularly evident in the dry period toward the end of 2017. As such, following the approach employed in Ref. [45], the deposition velocities were determined through a fitting process using the *curve_fit* function of the SciPy library [46]. The following boundaries were set: $v_{10-2.5} \geq v_{2.5} \geq 0$ cm/s. The best results were found for $v_{10-2.5} = v_{2.5} = 0.38$ cm/s. This is found to reduce the mean modelling error by more than 50%. The reduction in error reaches approximately 85% if only the higher soiling period in between July 2017 and June 2018 is considered.

The employed soiling estimation model is the most common one; it has been recently included among the pvlib-python functions [25] and it is currently also employed in commercial products [47]. However, it is acknowledged that the results of the models are exposed to an uncertainty, described in a previous work [48], due to the spatial resolution and to the type of data used as input. In addition, the modelled losses are not expected to reproduce local soiling conditions of any location, as these will vary depending on the microclimate and on the system's configuration as well. Rather, they provide an indication of the soiling trend within the country and identify the most and least soiled regions.

3. Results and discussion

3.1. Magnitude of clipping

Fig. 4 shows the impact that the inverter undersizing has on the PV energy yield in the contiguous U.S. In both fixed and tracked configurations, clipping is found to mainly occur in the non-coastal Southwestern states (see Fig. S 1 for a map of the U.S. states): Arizona, Colorado, Nevada, New Mexico, and Utah. This geographical distribution of clipping occurrence is due to the higher solar resource compared to the eastern states and to the lower temperature and lower soiling compared to the coastal west.

Fixed and HSAT systems in these states clip for more than 7% and 8% of the time, respectively. Colorado and New Mexico are the two states in which clipping occurs the most, with averages above 8% in both mounting configurations. By calculating a simple arithmetic mean, an average national clipping time of 4.0% and 3.5% per year can be estimated for fixed and HSAT PV systems, respectively.

However, the national average clipping time is actually higher if the uneven distribution of capacity across states is considered. A weighted average can be calculated by multiplying the average clipping time in each state to the state-specific PV capacity. More than 25% of the national capacity in 2019 was indeed installed in one of the previously mentioned high clipping states. If California is also included in this group, the percentage rises to 49%. Consequently, a weighted clipping time average of 4.6%–4.7% per year is obtained. The high value is due to the higher capacity concentrated in high solar insolation regions, when clipping occurs more frequently.

The weighted average returns a reduced difference between fixed tilt and HSAT systems as compared to the simple average. The reason for this is shown in the left plot of Fig. 4, where states with the heaviest clipping were found to exhibit similar clipping times for both fixed and HSAT configurations. These results can be attributed to the higher irradiance levels registered in these states, which increase the overall energy yield and the likeliness of clipping independently of the configuration. Fig. 5 showcases power output profiles and clipping behaviours on a representative day for a fixed tilt and a HSAT system installed south of Denver (Colorado). It can be observed that once clipping occurs, HSAT tend to experience it for more hours per day compared to fixed systems. On the other hand, fixed tilt systems are more likely to clip on a given day because they reach higher maximum power outputs at peak hours. This is due to their inclination, which lowers the angle of incidence around noon compared to HSAT systems in the sunniest months. However, their fixed-tilt daily power output profiles are narrower, with rapid increases and decreases occurring in just a few hours. Conversely, HSAT power production peaks at lower values and remain high for more hours. Therefore, fixed tilt systems are found to clip more frequently at least once a day in lower yield locations, as they are more prone to reaching inverter saturation conditions with their higher power peaks, even if only for short times. On the other hand, in areas with higher irradiance, HSAT systems are more likely to experience clipping for extended durations each day compared to fixed tilt systems. In other words, fixed tilt systems are more likely to clip because they have higher power peaks that can saturate the inverter, thanks to their lower angle of incidence at noon. The angles of incidence of HSAT systems, on the other hand, are higher at noon, but averagely lower throughout the day. This means that HSAT systems have lower power peaks that are spread out over a longer period of time, making them less likely to clip, but exposing them to longer clipping time once clipping conditions are reached.

While the percentage of clipping hours can be occasionally higher in HSAT, fixed-tilt systems are found to consistently mask a larger portion of energy (Fig. 4). On average, 1.4% of the DC energy is clipped in fixed-

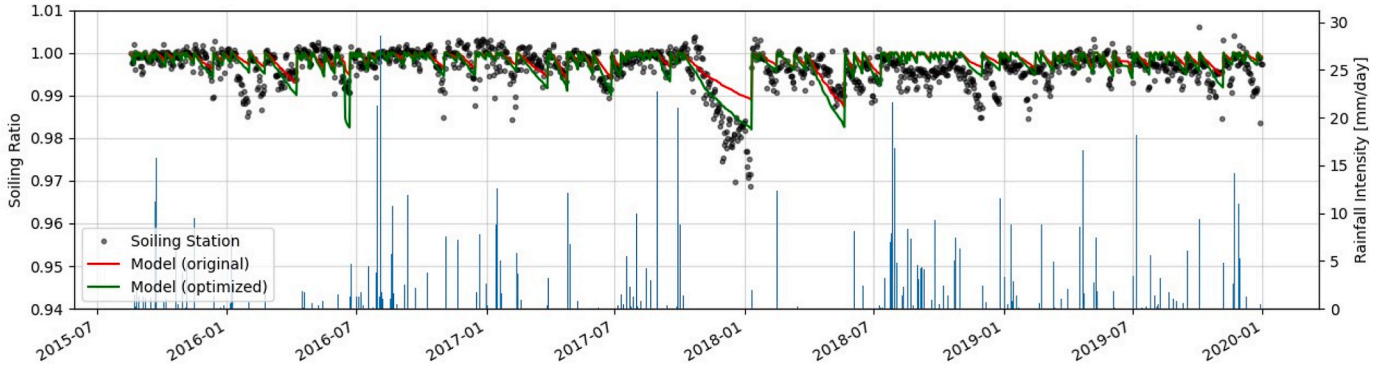

Fig. 3. Measured vs. modelled soiling ratio profiles at Sandia National Laboratories, NM, USA. The original model uses the settling velocities proposed by Ref. [41]. *The optimized model uses velocities obtained through a fitting process.*

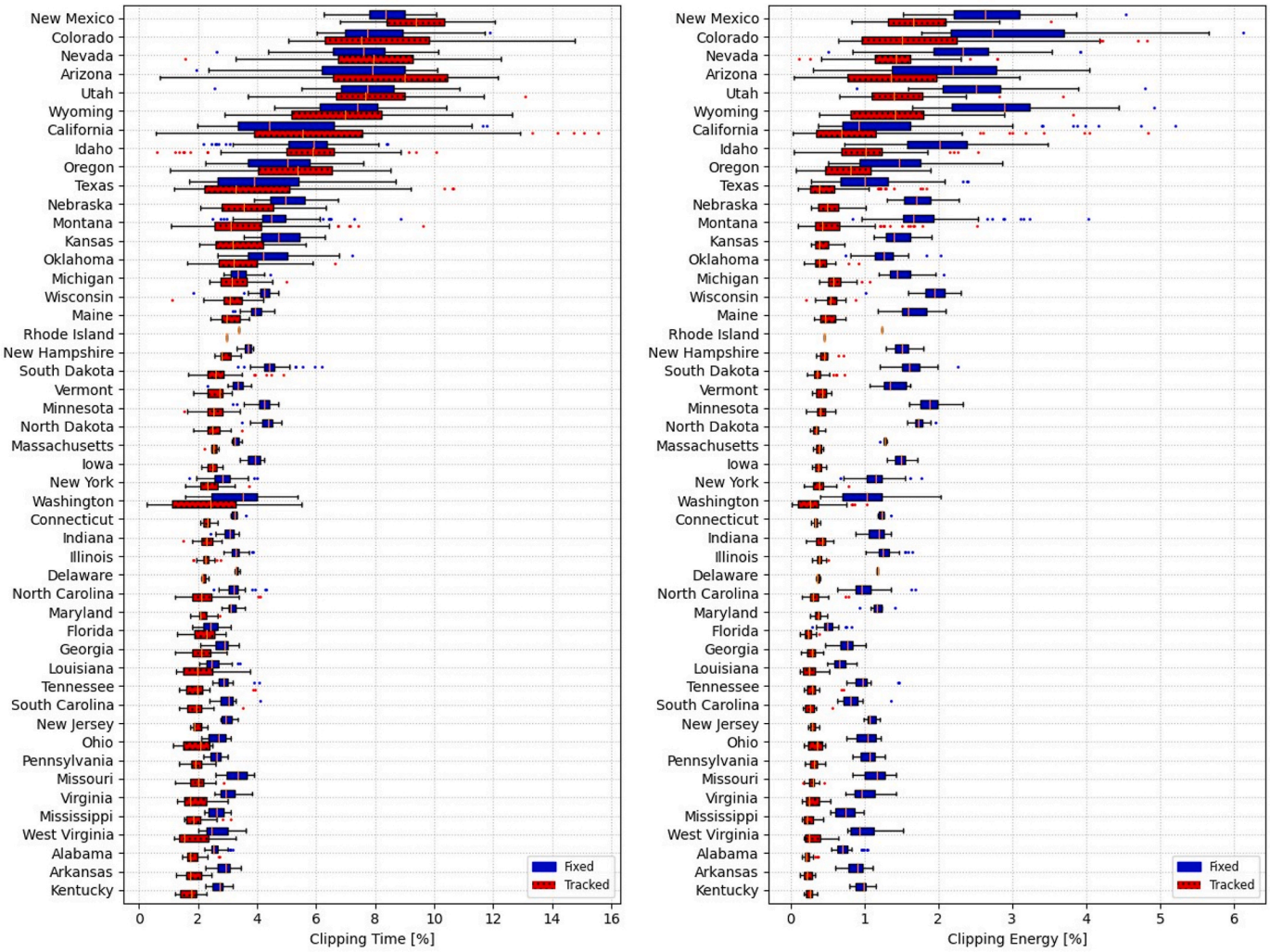

Fig. 4. Comparison of clipping time (left) and clipping energy (right) per state, depending on mounting configuration and assuming an ILR of 1.34. A map, with the location and the border of each state is reported in Fig. S 1.

tilt systems; this reduces to 0.6% in HSAT systems. This result is not surprising. Indeed, on average, at national level, HSAT systems produce almost 15% more energy than latitude-fixed systems. However, HSAT maximum hourly yields are about 10% lower. The higher energy generation is mainly due to the better performance in the mornings and in the afternoons compared to fixed systems.

Indeed, as can be seen in Fig. 5, the HSAT system produces more energy throughout the day as compared to fixed systems but have lower peaks at noon. On the other hand, the fixed tilt system has a higher peak power compared to the HSAT system (+4% without clipping) due to the closer-to-optimal inclination at noon. However, its power production is limited to the central hours of the day. Conversely, the HSAT system works for more hours at higher power outputs, resulting in a higher daily energy yield (+30% without clipping). Because of this flatter profile, clipping occurs for more hours in the HSAT system, explaining again some of the results shown in Fig. 4. On the other hand, however, even if the absolute amount of clipped energy is higher than in fixed systems (+90%), the relative amount is lower (−2%), because of the higher DC energy yield.

3.2. Impact of clipping on soiling

Soiling unevenly impacts the contiguous U.S. territories. Indeed, most of the losses take place in the Southwest, which are characterized by higher particulate matter concentrations and longer and drier summers. As show in Fig. 6a and b, and in agreement with previous literature and the NREL soiling map [48,49], soiling is found to cause the loss of up to 4% of the yearly energy yield in these regions, with peaks higher than 8% in some locations of Arizona. In the rest of the country, losses are typically limited to less than 2%/year.

At national level, inverter clipping reduces the visible soiling losses by less than 0.1 $\%_{abs}$, on average (Fig. 6c and d). This means that clipping can only partially contribute to mitigate soiling losses (Fig. 6e and f). The larger relative reduction in losses is indeed found in those areas where losses are already limited. For example, the highest relative reductions are found in New Mexico and Colorado (>40$\%_{rel}$), where, however, the soiling losses are not greater than 1.15 %/year and 0.6 %/year, respectively. On the other hand, in those areas where soiling losses are more intense, such as southern California and Arizona, the impact of clipping is limited. Indeed, the maximum absolute reduction in soiling losses does not exceed 1$\%_{abs}$, even in those locations where the losses are higher than 4%, and can reach up to 9%/year.

The limited mitigation that the inverter undersizing provides to soiling in the current PV deployment configuration trends can be explained by at least two factors, depicted also, for a representative location in California, in Fig. S 2 (Supplemental Material). The first one is the limited amount of clipped energy occurring in California and Arizona, despite the high inverter loading ratio. This is particularly true for HSAT systems for the reasons expressed above, and also shown in Fig. 4. The effect on soiling however is even weaker for fixed systems.

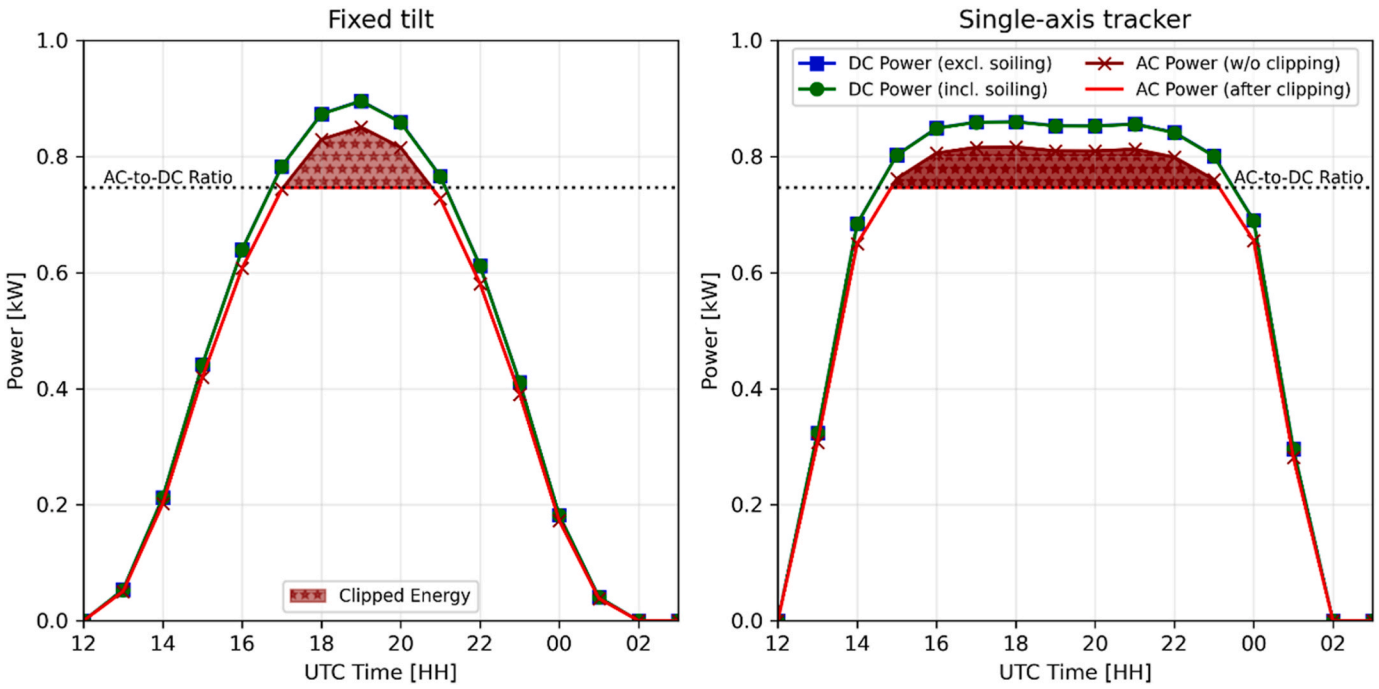

Fig. 5. Comparing the performance and the clipping mechanisms of a fixed-latitude-tilt and a HSAT PV system at the same location (Douglas County, CO) and on the same day (May 4th, 2018).

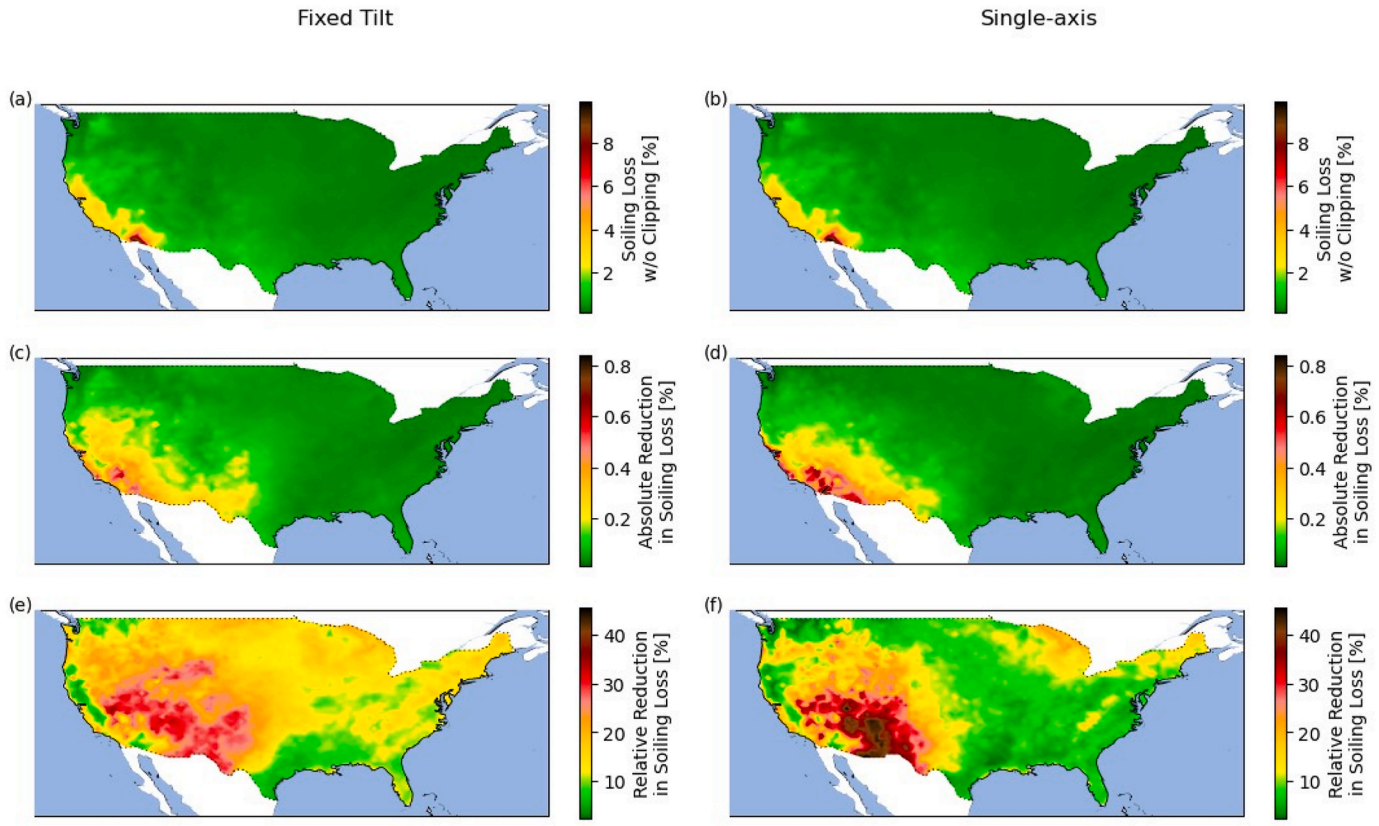

Fig. 6. Magnitude of the yearly soiling losses without considering clipping (a–b), absolute reduction in soiling losses due to clipping (c–d), and relative reduction in soiling losses due to clipping (e–f). Left plots (a, c, e) and right plots (b, d, f) correspond to fixed tilt and HSAT systems, respectively.

This is due to a mismatch between the seasons in which clipping and soiling occur. This can be clearly seen in Fig. 7, which reports the soiling and clipping profiles for the most soiled locations across the U.S. In optimally tilted fixed systems, clipping, indeed, mainly occurs in spring, when temperatures are milder and the solar elevation at noon is not at its peak. On the other hand, soiling mainly builds up during the dry, hot

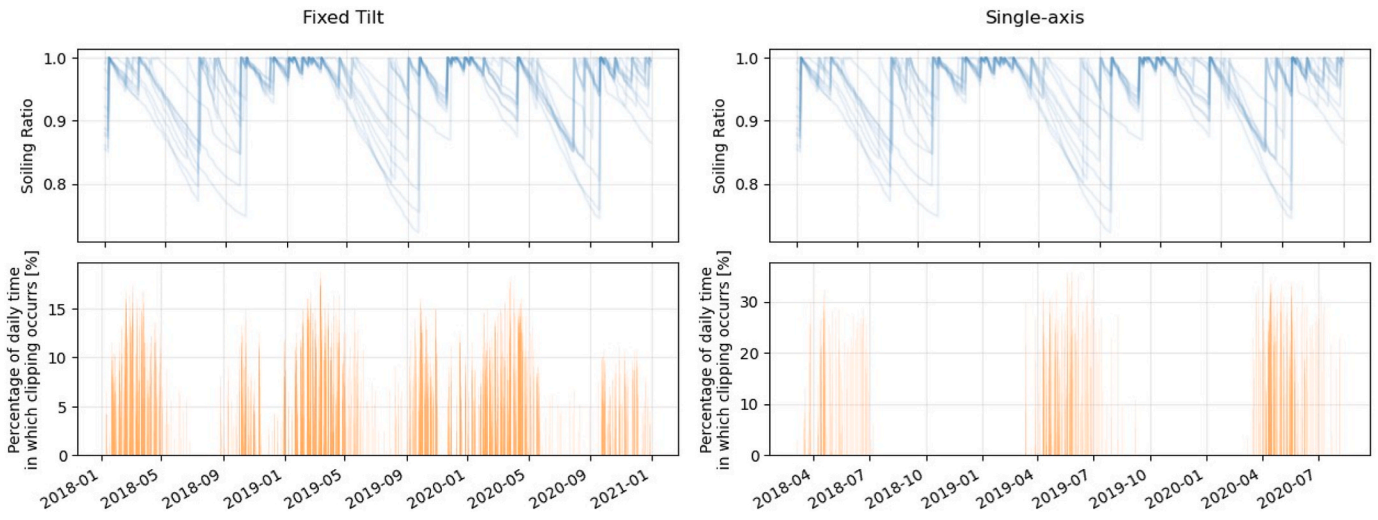

Fig. 7. Top plots: daily soiling ratio profiles. Bottom plots: percentage of time in which systems clips on each day. All the plots only show data for sites with losses higher than 4%/year, and all share the same x-axis.

summer, reaching its maximum towards September.

Fig. 7 also explains why the soiling reduction effect is higher in HSAT systems compared to fixed systems. The seasonal mismatch found for fixed systems does not occur for HSAT ones. Indeed, because of their horizontal position at noon, HSAT modules experience higher angular/reflection losses during spring compared to summer. In summer, indeed, the solar elevation is higher, reducing the angle of incidence and maximizing the energy yield during the central hours of the day. For this reason, both soiling and clipping of HSAT systems typically occur in summer, granting a higher loss mitigation effects compared to fixed systems.

So far, the analysis considered PV systems at their initial conditions. However, one should also take into account that PV modules and systems experience irreversible performance losses over their lifetime, which are a result of various degradation mechanisms [50]. These gradually lower the conversion efficiency of PV modules, meaning that, under the same conditions, modules are able to generate lower energy yields. This also means that, over time, clipping becomes less frequent.

An example of this gradual reduction in energy yield is shown in Fig. S 3, in the Supplemental Material, which depicts the same energy yield profile at years 1, 5 and 10 after installation. Because of degradation, the profile gradually decreases and the clipping conditions occur less frequently as the system ages. As shown, after 10 years, the selected PV site clips half the energy than it did originally. The results of this same analysis repeated for all the investigated locations are reported in Fig. 8. Assuming a linear performance loss rate of −0.75%/year and an inverter loading ratio of 1.34, most HSAT systems will not experience any clipping after 20 years. This time interval is longer for fixed systems (36 years) because of the aforementioned higher power peaks. This decreasing clipping occurrence makes the impact of soiling more intense as the oversized DC capacity ages. Indeed, the limited clipping due to the system aging means that, even when they were originally masked, soiling losses would become more visible on the AC side with time. For these reasons, one should take into account that, even in case of significant clipping-related mitigation, soiling could become more significant with time because of degradation.

3.3. Discussion

Overall, the results show that a 1.34 ILR was not able to substantially mitigate the peak soiling losses that occur in the Southwestern U.S. However, it is acknowledged that these results might change depending on factors such as the losses experienced by the PV systems and the designed inverter undersizing. For this reason, two additional scenarios were modelled by varying ILR from 1.26 to 1.45 (i.e., the 20th and 80th percentiles reported in Ref. [12]), and the DC to AC losses from 5% to 15%. The first scenario assumes high clipping conditions: higher ILR (1.45) and lower losses (5%). On the other hand, the second scenario assumes less frequent clipping conditions: lower ILR (1.26) and higher PV performance losses (15%).

As expected, in the first scenario, the occurrence of clipping and the overall effects of inverter undersizing become more significant. The average clipping time rises to 8.6% and 10.5% in fixed and HSAT configurations, respectively. If the weighted average is considered, these values become 10.3% and 12.9%. In this scenario, between 4% and 5% of the DC energy is clipped. Due to the most frequent clipping occurrences, the soiling mitigation effect becomes more substantial, with maximum loss reductions up to 3% (Fig. 9). As such, in this case, soiling losses can be almost halved even in the southwestern regions and in those locations exposed to higher losses. Under these clipping prone

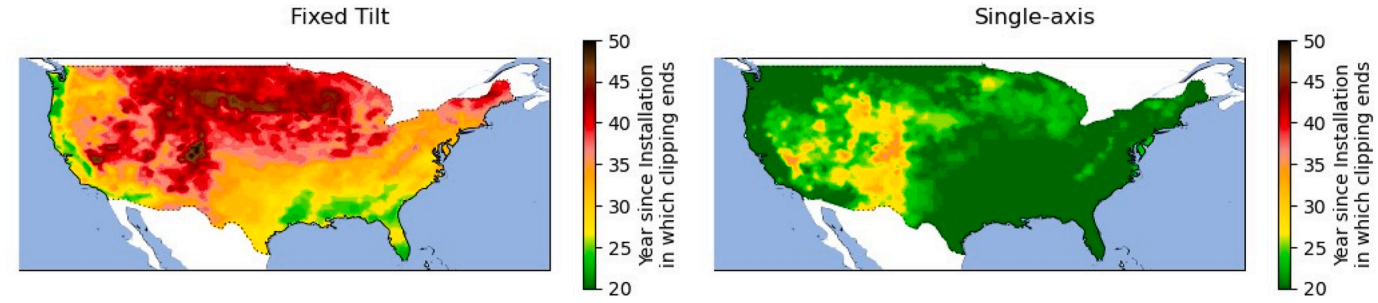

Fig. 8. Number of years until clipping stops, assuming a linear performance loss rate of −0.75%.

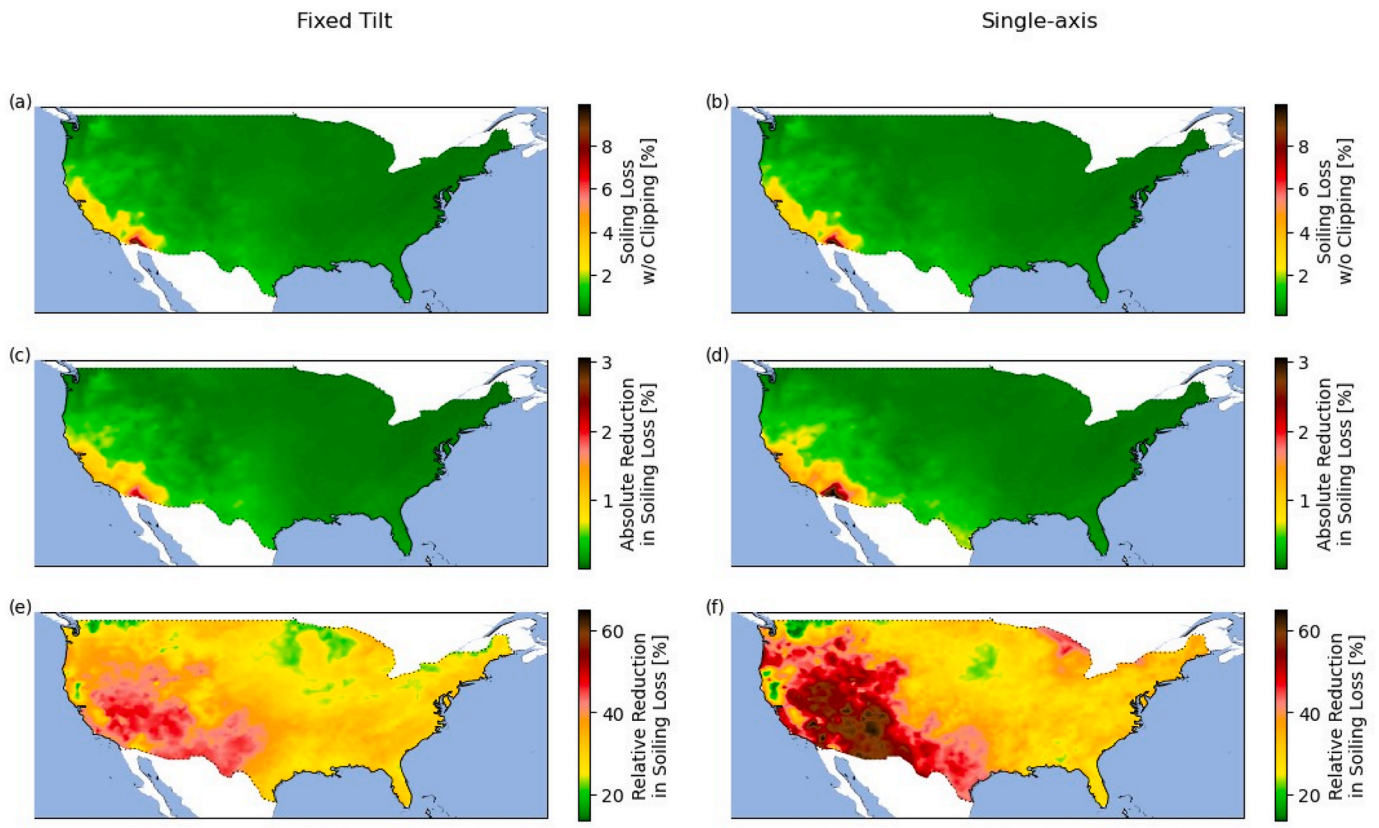

Fig. 9. Magnitude of the yearly soiling losses without considering clipping (a–b), absolute reduction in soiling losses due to clipping (c–d), and relative reduction in soiling losses due to clipping (e–f) under the most clipping prone scenario (ILR: 1.45, performance losses: 5%). Left plots (a, c, e) and right plots (b, d, f) correspond to fixed tilt and HSAT systems, respectively.

conditions, the effect of inverter undersizing would last for a period of 30–50 years and 17–48 years for the fixed tilt and HSAT configuration, respectively, with most of locations experiencing no clipping after 40.5 years and 30 years.

On the other hand, as expected, the conditions modelled in the second scenario led to a significant drop in the effect of inverter undersizing. In this case, the clipping time drops below 1% in all configurations, with a percentage of clipped energy not higher than 0.2%. This means that the soiling mitigation effect is even lower than in the reference scenario, with absolute reductions of 0.1% $_{abs}$ or less and relative reductions up to approximately 15%$_{rel}$ (Fig. S 5).

As previously mentioned, an additional factor that impacts the clipping frequency is the performance loss rate. This value itself has been reported to be affected by a number of factors, including, for example, the PV technology [51], and the climate [52]. However, variations in the performance loss rates are expected to have repercussions also on the results shown in this work. For this reason, a sensitivity analysis was also conducted on the performance loss rate, which, in the reference scenario, was set to a linear −0.75%/year value. Therefore, the same analysis shown in the previous subsections was repeated, assuming first a more severe performance loss rate of −1%/year, close to that experienced in harsher climates [33], and then a slower rate of −0.5 %/year, typical of cooler climates, according to Ref. [33]. Under the worst performance loss rate, most systems will not experience any clipping after 24 years in fixed tilt configuration and after 14 years in HSAT. These periods become longer, as expected, if a slower loss rate is considered; 48 and 28 years, respectively. Therefore, it is important to highlight again that, even if clipping is initially able to effectively mask (part of) the soiling losses, the mitigation effect would become weaker with time.

Overall, the findings of this work confirm that relying solely on a high inverter-loading ratio (ILR) may not be sufficient to effectively mitigate soiling losses, especially over the long-term. Soiling mitigation, indeed, can be expected to become increasingly important and more economically viable as the system ages. This means that, in practical terms, there may be a growing need to invest in soiling mitigation as the system ages. During the PV system design phase, the expected impact of clipping over the whole PV system lifetime should be assessed, taking into account the specific characteristics of the system and the inverter, as well as the anticipated soiling losses. In the operational phases, soiling should be regularly monitored in order to assess whether anti-soiling actions, such as periodic cleanings, should be put in place, independent of the initial mitigating effects of inverter undersizing.

The present analysis focuses on clipping and soiling occurring across the contiguous United States. However, it should be highlighted that the goal of this work is not to provide an overview on the status of soiling and clipping for a specific country, but rather to evaluate whether clipping can be considered an effective soiling mitigation technique. To do that, the correlation between these two phenomena was studied using the actual conditions of a selected region. However, these can be considered representative of a variety of locations. Specifically, more than 20 diverse climates can be identified in the contiguous United States territory [20–22], as shown in Fig. S 4. For example, the desert climate (BWh and BWk), common in the Southwestern-most part of the United States, is typical of North Africa, central/interior Australia, and northern Chile, some of the regions with the highest solar potential and most significantly exposed to soiling. Semi-arid climates (BSh and BSk), also found in the southwest of the U.S., is common in Spain and Australia, both regions of high PV penetration. At the same time, the soiling losses registered in the southwestern U.S. are common to many locations worldwide [1], including most of Europe, Australia, and the rest of the American continent [53].

4. Conclusions

The present work investigates the theoretical impact of inverter undersizing on the PV energy production and on the soiling losses across the U.S. It is found that, for the current typical 1.34 inverter loading ratio and a fixed 10% PV loss, systems clip, on average, 3.5–4.0% of the time each year. Most of the clipping occurs in the non-coastal Southwestern states, where the solar potential is high, the temperatures are milder, and soiling is limited. Overall, however, clipping masks only a small percentage (<2%) of the annual DC energy yield. HSAT systems are found to have a smaller portion of energy masked by clipping compared to fixed systems.

It is found that, under the reference conditions modelled in this work, inverter undersizing has only limited effect on the severity of soiling losses across the contiguous United States. On average, for a 1.34 inverter loading ratio, the inverter undersizing reduces the visible soiling losses by no more than $1\%_{abs}$. A stronger soiling mitigation is found in those locations already experiencing low-to-intermediate losses.

It must be acknowledged that any variation in the modelled conditions (i.e., ILR = 1.34, 10% DC to AC losses and 95%-efficient inverter), could change the magnitude of the results, as shown by the reported sensitivity analysis. Nonetheless, even if soiling is initially mitigated by the inverter undersizing, the losses would become more visible with time, as degradation makes clipping less frequent, therefore reducing the masking effect.

Overall, the analysis suggests that the PV operators should not fully rely on the undersizing of the inverter as a universally effective anti-soiling solution in the Southwest of the U.S. However, because of the constantly varying PV configurations and in light of the results of the presented sensitivity analysis, future studies should revise the current findings taking into account the most up-to-date models and most recent industry trends.

Data sharing

The data that support the findings of this study are available from the corresponding author upon reasonable request.

CRediT authorship contribution statement

Leonardo Micheli: Writing – original draft, Visualization, Validation, Software, Methodology, Investigation, Formal analysis, Data curation, Conceptualization. **Matthew Muller:** Writing – review & editing, Validation, Methodology, Investigation, Data curation. **Marios Theristis:** Writing – review & editing, Methodology, Investigation, Data curation. **Greg P. Smestad:** Writing – review & editing, Methodology. **Florencia Almonacid:** Writing – review & editing. **Eduardo F. Fernández:** Writing – review & editing.

Declaration of competing interest

The authors declare that they have no known competing financial interests or personal relationships that could have appeared to influence the work reported in this paper.

Acknowledgments

The authors wish to thank Dan Riley, Sandia National Laboratories, for providing the soiling station data.

L. Micheli's work was supported by Sole4PV, a project funded by the Italian Ministry of University and Research under the "Rita Levi di Montalcini" 2019 grant.

The work of M. Muller was supported by the Alliance for Sustainable Energy, LLC, the manager and operator of the National Renewable Energy Laboratory for the U.S. Department of Energy (DOE) under Contract No. DE-AC36-08GO28308. Funding provided by the U.S. Department of Energy's Office of Energy Efficiency and Renewable Energy (EERE) under Solar Energy Technologies Office (SETO) Agreement Number 38258. The views expressed in the article do not necessarily represent the views of the DOE or the U.S. Government. The U.S. Government retains and the publisher, by accepting the article for publication, acknowledges that the U.S. Government retains a nonexclusive, paid-up, irrevocable, worldwide license to publish or reproduce the published form of this work, or allow others to do so, for U.S. Government purposes.

The work of M. Theristis was supported by the U.S. Department of Energy's Office of Energy Efficiency and Renewable Energy (EERE) under the Solar Energy Technologies Office Award Number 38267. Sandia National Laboratories is a multimission laboratory managed and operated by National Technology & Engineering Solutions of Sandia, LLC, a wholly owned subsidiary of Honeywell International Inc., for the U.S. Department of Energy's National Nuclear Security Administration under contract DE-NA0003525. This article describes objective technical results and analysis. Any subjective views or opinions that might be expressed in this article do not necessarily represent the views of the U.S. Department of Energy or the Unites States Government.

E.F. Fernández thanks the Spanish Ministry of Science, Innovation and Universities for the funds received under the "Ramón y Cajal Programme" (RYC-2017-21910).

Appendix A. Supplementary data

Supplementary data to this article can be found online at https://doi.org/10.1016/j.renene.2024.120317.

References

[1] M.M.H. Mithhu, T.A. Rima, M.R. Khan, Global analysis of optimal cleaning cycle and profit of soiling affected solar panels, Appl. Energy 285 (2021), https://doi.org/10.1016/j.apenergy.2021.116436.

[2] K. Chiteka, R. Arora, S.N. Sridhara, C.C. Enweremadu, Optimizing wind barrier and photovoltaic array configuration in soiling mitigation, Renew. Energy 163 (2021) 225–236, https://doi.org/10.1016/j.renene.2020.08.155.

[3] K. Ilse, M.Z. Khan, N. Voicu, V. Naumann, C. Hagendorf, J. Bagdahn, Advanced performance testing of anti-soiling coatings – Part I: sequential laboratory test methodology covering the physics of natural soiling processes, Sol. Energy Mater. Sol. Cells 202 (2019) 110048, https://doi.org/10.1016/j.solmat.2019.110048.

[4] B.W. Figgis, K.K. Ilse, Anti-soiling potential of 1-Axis PV trackers, 36th, Eur. Photovolt. Sol. Energy Conf. Exhib. (2019) 1312–1316, https://doi.org/10.4229/EUPVSEC20192019-5BO.7.1.

[5] R. Conceição, I. Vázquez, L. Fialho, D. García, Soiling and rainfall effect on PV technology in rural Southern Europe, Renew. Energy 156 (2020) 743–747, https://doi.org/10.1016/j.renene.2020.04.119.

[6] L. Cristaldi, M. Faifer, M. Rossi, M. Catelani, L. Ciani, E. Dovere, et al., Economical evaluation of PV system losses due to the dust and pollution, in: 2012 IEEE I2MTC - Int. Instrum. Meas. Technol. Conf. Proc., 2012, pp. 614–618, https://doi.org/10.1109/I2MTC.2012.6229521.

[7] R.K. Jones, A. Baras, A. Al Saeeri, A. Al Qahtani, A.O. Al Amoudi, Y. Al Shaya, et al., Optimized cleaning cost and schedule based on observed soiling conditions for photovoltaic plants in Central Saudi Arabia, IEEE J. Photovoltaics 6 (2016) 730–738, https://doi.org/10.1109/JPHOTOV.2016.2535308.

[8] P. Besson, C. Munoz, G. Ramirez-Sagner, M. Salgado, R. Escobar, W. Platzer, Long-term soiling analysis for three photovoltaic Technologies in santiago region, IEEE J. Photovoltaics 7 (2017) 1755–1760, https://doi.org/10.1109/JPHOTOV.2017.2751752.

[9] E.G. Luque, F. Antonanzas-Torres, R. Escobar, Effect of soiling in bifacial PV modules and cleaning schedule optimization, Energy Convers. Manag. 174 (2018) 615–625, https://doi.org/10.1016/j.enconman.2018.08.065.

[10] S. You, Y.J. Lim, Y. Dai, C.H. Wang, On the temporal modelling of solar photovoltaic soiling: energy and economic impacts in seven cities, Appl. Energy 228 (2018) 1136–1146, https://doi.org/10.1016/j.apenergy.2018.07.020.

[11] J. Balfour, R. Hill, A. Walker, G. Robinson, T. Gunda, J. Desai, et al., Masking of photovoltaic system performance problems by inverter clipping and other design and operational practices, Renew. Sustain. Energy Rev. 145 (2021) 111067, https://doi.org/10.1016/j.rser.2021.111067.

[12] M. Bolinger, J. Seel, C. Warner, D. Robson, Utility-Scale Solar, 2021 Edition, 2021. Berkeley, CA, USA, http://utilityscalesolar.lbl.gov.

[13] H.X. Wang, M.A. Muñoz-García, G.P. Moreda, M.C. Alonso-García, Optimum inverter sizing of grid-connected photovoltaic systems based on energetic and economic considerations, Renew. Energy 118 (2018) 709–717, https://doi.org/10.1016/j.renene.2017.11.063.

[14] G. Mütter, The practical impact of high DC/AC ratios on effective soiling loss, in: PVQAT Task Group 12, Eff. DCAC Ratio Soiling Loss Degrad., PVQAT Task Group 12, 2019.
[15] National Renewable Energy Laboratory, National Solar Radiation Data Base (NSRDB), (n.d.). https://nsrdb.nrel.gov/(accessed May 18, 2018).
[16] PRISM Climate Group - Oregon State University, PRISM Climate Group - Oregon State University, (n.d.). http://www.prism.oregonstate.edu/explorer/(accessed May 14, 2019) .
[17] Global Modeling and Assimilation Office (GMAO), MERRA-2 tavg1_2d_slv_Nx: 2d,1-Hourly,Time-Averaged,Single-Level,Assimilation, Single-Level Diagnostics V5 12 (4) (2019), https://doi.org/10.5067/VJAFPLI1CSIV.
[18] Global Modeling and Assimilation Office (GMAO), MERRA-2 tavg1_2d_aer_Nx: 2d,1-Hourly,Time-averaged,Single-Level,Assimilation, Aerosol Diagnostics 0.625 x 0.5 degree V5.12.4 (M2T1NXAER) (2020). https://goldsmr4.gesdisc.eosdis.nasa.gov/opendap/MERRA2/M2T1NXAER.5.12.4/. (Accessed 6 November 2020).
[19] Met Office (UK), Cartopy v0.11.2. 22. https://github.com/SciTools/cartopy/archive/v0.11.2.tar.gz%0A, 2020. (Accessed 21 April 2021).
[20] W. Koppen, E. Volken, S. Bronnimann, The thermal zones of the Earth according to the duration of hot, moderate and cold periods and to the impact of heat on the organic world, Meteorol. Z. 20 (2011) 351–360, https://doi.org/10.1127/0941-2948/2011/105.
[21] F. Rubel, M. Kottek, Observed and projected climate shifts 1901-2100 depicted by world maps of the Köppen-Geiger climate classification, Meteorol. Z. 19 (2010) 135–141, https://doi.org/10.1127/0941-2948/2010/0430.
[22] F. Rubel, K. Brugger, K. Haslinger, I. Auer, The climate of the European Alps: shift of very high resolution Köppen-Geiger climate zones 1800-2100, Meteorol. Z. 26 (2017) 115–125, https://doi.org/10.1127/metz/2016/0816.
[23] X. Yu, C. Bryant, N.R. Wheeler, F. Rubel, J.A. Vasquez, R.H. French, kgcPy, 2023, 1.1.3.
[24] A.P. Dobos, PVWatts Version 5 Manual, 2014. https://pvwatts.nrel.gov/downloads/pvwattsv5.pdf.
[25] W.F. Holmgren, C.W. Hansen, M.A. Mikofski, Pvlib python: a python package for modeling solar energy systems, J. Open Source Softw. 3 (2018), https://doi.org/10.21105/joss.00884.
[26] P.G. Loutzenhiser, H. Manz, C. Felsmann, P.A. Strachan, T. Frank, G.M. Maxwell, Empirical validation of models to compute solar irradiance on inclined surfaces for building energy simulation, Sol. Energy 81 (2007) 254–267, https://doi.org/10.1016/j.solener.2006.03.009.
[27] R. Perez, P. Ineichen, R. Seals, J. Michalsky, R. Stewart, Modeling daylight availability and irradiance components from direct and global irradiance, Sol. Energy 44 (1990) 271–289.
[28] D.L. King, W.E. Boyson, J.A. Kratochvill, Photovoltaic Array Performance Model, 2004, https://doi.org/10.2172/919131. Albuquerque, New Mexico.
[29] Trina, Vertex TSM-DE20 585-605W, 2021. https://static.trinasolar.com/sites/default/files/EN_Datasheet_Vertex_DE20_202103A.pdf.
[30] W. De Soto, S.A. Klein, W.A. Beckman, Improvement and validation of a model for photovoltaic array performance, Sol. Energy 80 (2006) 78–88, https://doi.org/10.1016/j.solener.2005.06.010.
[31] E. Lorenzo, L. Narvarte, J. Muñoz, Tracking and back-tracking, Prog. Photovoltaics Res. Appl. 19 (2011) 747–753, https://doi.org/10.1002/pip.1085.
[32] A.P. Dobos, PVWatts Version 5 Manual (NREL/TP-6A20-62641), Natl. Renew. Energy Lab., 2014, p. 20.
[33] D.C. Jordan, K. Anderson, K. Perry, M. Muller, M. Deceglie, R. White, et al., Photovoltaic fleet degradation insights, Prog. Photovoltaics Res. Appl. 30 (2022) 1166–1175, https://doi.org/10.1002/pip.3566.
[34] K. Perry, M. Muller, K. Anderson, Performance comparison of clipping detection techniques in AC power time series, Conf. Rec. IEEE Photovolt. Spec. Conf. (2021) 1638–1643, https://doi.org/10.1109/PVSC43889.2021.9518733.
[35] M. Theristis, N. Riedel-Lyngskær, J.S. Stein, L. Deville, L. Micheli, A. Driesse, et al., Blind photovoltaic modeling intercomparison: a multidimensional data analysis and lessons learned, Prog. Photovoltaics Res. Appl. (2023) 1–14, https://doi.org/10.1002/pip.3729.
[36] IEA PVPS Task 13, Uncertainties in Yield Assessments and PV LCOE, 2020.
[37] D. Yang, Validation of the 5-min irradiance from the national solar radiation database (NSRDB), J. Renew. Sustain. Energy 13 (2021), https://doi.org/10.1063/5.0030992.
[38] J. Good, J.X. Johnson, Impact of inverter loading ratio on solar photovoltaic system performance, Appl. Energy 177 (2016) 475–486, https://doi.org/10.1016/j.apenergy.2016.05.134.
[39] R. Kharait, S. Raju, A. Parikh, M.A. Mikofski, J. Newmiller, Energy yield and clipping loss corrections for hourly inputs in climates with solar variability, Conf. Rec. IEEE Photovolt. Spec. Conf. (2020) 1330–1334, https://doi.org/10.1109/PVSC45281.2020.9300911, 2020-June.
[40] K. Anderson, K. Perry, Estimating subhourly inverter clipping loss from satellite-derived irradiance data, Conf. Rec. IEEE Photovolt. Spec. Conf. (2020) 1433–1438, https://doi.org/10.1109/PVSC45281.2020.9300750, 2020-June.
[41] M. Coello, L. Boyle, Simple model for predicting time series soiling of photovoltaic panels, IEEE J. Photovoltaics 9 (2019) 1382–1387, https://doi.org/10.1109/JPHOTOV.2019.2919628.
[42] NASA, MERRA-2 FAQ, (n.d.). https://gmao.gsfc.nasa.gov/reanalysis/MERRA-2/FAQ/(accessed June 10, 2021).
[43] S. Provençal, V. Buchard, M. Arlindo, R. Leduc, N. Barrette, Evaluation of PM surface concentrations simulated by version 1 of NASA ' s MERRA aerosol reanalysis over Europe, Atmos. Pollut. Res. 8 (2017) 374–382, https://doi.org/10.1016/j.apr.2016.10.009.
[44] J. Zorrilla-Casanova, M. Piliougine, J. Carretero, P. Bernaola-Galván, P. Carpena, L. Mora-López, et al., Losses produced by soiling in the incoming radiation to photovoltaic modules, Prog. Photovoltaics Res. Appl. 21 (2013) 790–796, https://doi.org/10.1002/pip.1258.
[45] S. Toth, M. Hannigan, M. Vance, M. Deceglie, Predicting photovoltaic soiling from air quality measurements, IEEE J. Photovoltaics 10 (2020) 1142–1147, https://doi.org/10.1109/JPHOTOV.2020.2983990.
[46] E. Jones, E. Oliphant, P. Peterson, et al., SciPy: Open Source Scientific Tools for Python, 2001. http://www.scipy.org/.
[47] SolarAnywhere, Soiling-loss Modeling, (n.d.). https://www.solaranywhere.com/support/solar-energy-modeling-services/soiling-loss-modeling/ (accessed June 30, 2021).
[48] L. Micheli, G.P. Smestad, J.G. Bessa, M. Muller, E.F. Fernandez, F. Almonacid, Tracking soiling losses: assessment, uncertainty, and challenges in mapping, IEEE J. Photovoltaics 12 (2022) 114–118, https://doi.org/10.1109/JPHOTOV.2021.3113858.
[49] National Renewable Energy Laboratory, Photovoltaic Modules Soiling Map, 2018. https://www.nrel.gov/pv/soiling.html. (Accessed 18 May 2018).
[50] M. Aghaei, A. Fairbrother, A. Gok, S. Ahmad, S. Kazim, K. Lobato, et al., Review of degradation and failure phenomena in photovoltaic modules, Renew. Sustain. Energy Rev. 159 (2022) 112160, https://doi.org/10.1016/j.rser.2022.112160.
[51] D.C. Jordan, S.R. Kurtz, K.T. VanSant, J. Newmiller, Compendium of photovoltaic degradation rates, Prog. Photovoltaics Res. Appl. 24 (2016) 978–989, https://doi.org/10.1002/pip.2744.
[52] J. Ascencio-Vásquez, I. Kaaya, K. Brecl, K.A. Weiss, M. Topič, Global climate data processing and mapping of degradation mechanisms and degradation rates of PV modules, Energies 12 (2019) 1–16, https://doi.org/10.3390/en12244749.
[53] X. Li, D.L. Mauzerall, M.H. Bergin, Global reduction of solar power generation efficiency due to aerosols and panel soiling, Nat. Sustain. 3 (2020) 720–727, https://doi.org/10.1038/s41893-020-0553-2.